# Afterpulse and dark count simulator for single photon avalanche detector

**Mahdi Rahmanpour**
Malek-Ashtar University of Technology
**Mahdi Khaje**
Malek-Ashtar University of Technology
**Alireza Erfanian** ( erfanian@mut.ac.ir )
Malek-Ashtar University of Technology
**MohammahHossein Fahimifar**
Malek-Ashtar University of Technology
**Ahmad Afifi**
Malek-Ashtar University of Technology

**Research Article**

**Keywords:** Single photon detector, Afterpulse, Dark count rate, Simulator, FPGA

**Posted Date:** July 20th, 2023

**DOI:** https://doi.org/10.21203/rs.3.rs-3175872/v1



**Additional Declarations:** Competing interest reported. Quantum single photon electronics photonics

# Afterpulse and dark count simulator for single photon avalanche detector


Mahdi Rahmanpour
*Faculty of Electrical and Computer Engineering, Malek-Ashtar University of Technology*
*Tehran, Iran*
rahmanpour@mut.ac.ir

Alireza Erfanian
*Faculty of Electrical and Computer Engineering, Malek-Ashtar University of Technology*
Tehran, Iran
erfanian@mut.ac.ir

Ahmad Afifi
*Faculty of Electrical and Computer Engineering, Malek-Ashtar University of Technology*
Tehran, Iran
afifi@mut.ac.ir

Mahdi Khaje
*Faculty of Electrical and Computer Engineering, Malek-Ashtar University of Technology*
Tehran, Iran
m.khaje@mut.ac.ir

MohammahHossein Fahimifar
*Faculty of Electrical and Computer Engineering, Malek-Ashtar University of Technology*
Tehran, Iran
fahimifar@mut.ac.ir



***Abstract*— Avalanche single photon detector detects the presence or absence of photons and their reception frequency. One of the most important challenges of using InGaAs semiconductor in single-photon detectors is detecting error pulses in two categories of dark counting and afterpulse counting. Dark counting is the revealing output pulses that are created in conditions of no photon reception. its leading cause is due to temperature effects on the carriers. Afterpulse is another undesirable factor that occurs due to the trapping of carriers after the avalanche failure event in the detector. The trapped carriers accelerate due to the electric field applied to the detector and create another avalanche breakdown called afterpulse. Due to the importance of the error resulting from dark and afterpulse counting in photon detection and the need to analyze, optimize and reduce its effects, it is necessary to simulate their behavior. In this article, a new method of simulating noise of SPADs is presented. In the proposed model, FPGA chip is used to generate error pulses. The proposed FPGA model is XC3S400 from Xilinx. By the VHDL hardware design code, the parameters effective in creating the dark pulse, and afterpulse are placed in their simulator equations. the results appear in the output as unwanted pulses next to the photon pulses.***



***Keywords: Single photon detector, Afterpulse, Dark count rate, Simulator, FPGA***


## I. INTRODUCTION

Single photon detection technology is a method that has been developed in recent years. it can detect photons as fragile light signals by various techniques[1].

In the 1960s, R.H. Haitz's working group proposed a new theory of avalanche breakdown in p-n junctions with a bias higher than the breakdown voltage. In the 1970s, R.J. Mcintyre and P.P. Webb observed single-photon pulses in photodiodes biased above the breakdown voltage. This event led to the development of the single photon avalanche breakdown diode. The SPAD[1] is a reverse-biased photodiode designed to operate in the region above the reverse-bias breakdown called the Geiger mode. In this region of bias, due to the high electric field, the reception of a single photon can cause an avalanche breakdown in the SPAD[2].

In Geiger mode, the SPAD is biased with an excess voltage ($V_{ex}$) beyond the breakdown voltage ($V_{BD}$) similar to the diagram in Figure (1). Therefore, the electric field in the discharge region is very high. by injecting an electron into the discharge region, it can lead to avalanche breakdown[3].

Semiconductor Single-Photon detectors are the second generation of Single-Photon devices that developed in the 1960s with the development of solid-state avalanche breakdown photodiodes with high breakdown voltage bias. Single-Photon detectors Have an increased sensitivity to the incident photon at a wavelength of 1550nm[3].

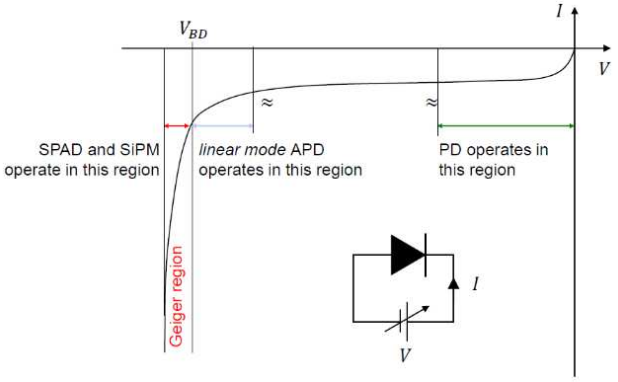


Fig 1. Photodiode working areas in reverse bias[4]

SPAD performance is affected by several important parameters: afterpulse probability, dark count rate, jitter amount, photon detection efficiency and temperature. These parameters are dependent on each other and at the same time, there is no complete mathematical model to show their dependence. A mathematical model is presented, combined with the existing circuit and physical model to produce a model of SPAD using Riccati's nonlinear differential equation. Modeling single photon detectors ensures their performance in the system. This model can calculate the output current, dark count rate, afterpulse probability, photon detection efficiency and amount of jitter produced by a single photon detector[3].

Table (1) presents the specifications of various types of single photon detector products produced by different companies.

[1] Single Photon Avalanche Diode

Table 1. Specifications of single photon detector types[5]

| SPD (company) | System efficiency | Dark count rate (cps) | Repetition rate | Working temperature |
|---|---|---|---|---|
| GaAs PMT (Hamamatsu) | 40%(580 nm) | 100 | 10 MHz | 230 K |
| Si APD (MPD) | 49%(550 nm) | 250 | 10 MHz | 300 K |
| Si APD (PerkinElmer) | 65%(650nm) | 25 | 10 MHz | 250 K |
| InGaAs/InP (ID Quantique) | 20%(1550 nm) | 10000 | 100 kHz | 260 K |
| TES (NIST) | 95%(1550 nm) | 3 | 100 kHz | 0.1 K |
| SSPD (Moscow) | 35%(1550 nm) | 10 | 70 MHz | 2 K |
| SSPD (MIT) | 23%(1550 nm) | 100 | 100 kHz | 1.8 K |
| SSPD (NICT) | 69%(1550 nm) | 100 | 50 MHz | 2.1 K |

SPAD gated-mode operation is a method for when no photons are expected to be received, and it reduces noise by turning off the detector. In this method, the photon pulses are set to be received during a time interval when the detector is biased above the breakdown voltage and turned on. The detector's on/off speed depends on its gate frequency[3].

## II. IMPLEMENTATION METHOD

### A. *Afterpulse*

When an avalanche occurs, the PN junction is filled with charge carriers, and the trap surface between the capacitance and the conduction band is occupied to a degree that is much more than expected in the thermal equilibrium distribution of charge carriers. After the SPAD is turned off, there is a possibility that a charge carrier in the depletion region will receive enough energy to be released and promoted to the conduction band, causing a new avalanche. Such carriers are released with long time constants (up to a few microseconds), and if one of the carriers is released while the SPAD is on, an avalanche may occur and lead to the afterpulse effect. Afterpulse is very important because it affects the linearity of the photon counting process and limits the maximum achievable counting rate[6].

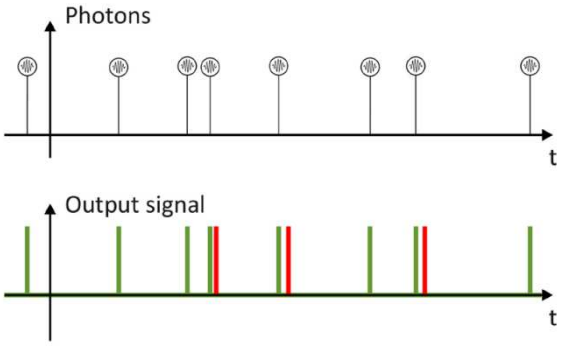


Fig 2. Afterpulse event[3]

The probability of afterpulse occurrence, which is defined as the ratio of the total number of afterpulses to the number of photons, is calculated from the following formula:

$$Pap=((I_{NI}-I_D)/(I_{Ph}-I_{NI}))R \quad (1)$$

$I_{Ph}$ is the count rate of each gate in light and $I_{NI}$ is no-light count. $I_D$ is the dark count rate for each gate, and R is the ratio of the repetition frequency of the gate pulse to the laser pulse[7].

The time interval during of the afterpulse is expressed by the sum of several exponential distributions. The time interval of afterpulse generation is calculated with the following equation[6]:

$$\Delta t_{AP} \propto \sum_k Ak \times exp\left(\frac{\Delta t}{\tau k}\right) \quad (2)$$

k: $\Delta t_{AP}$ number of time constants for afterpulse

Ak: constant value

τk: time constant of afterpulse generation

$$P_{ap}(t) = \sum_{i=1}^{N} A_i \frac{1}{\tau_i(E_i,T)} e^{-\frac{t}{\tau_i(E_i,T)}} \quad (3)$$

$$\tau_i(E_i,T) = \tau_0 e^{-\frac{E_i}{KT}} \quad (4)$$

i: pointer to Trap

$A_i$: is the probability of trap occurrence in avalanche failure

N: number of trapped carriers

$\tau_i(E_i,T)$: lifetime of a Trap

$E_i$: the activation energy of the trapped carrier

T: temperature

t: time

$\tau_0$: parameter dependent on carrier type

k: Boltzmann's constant

The afterpulse rate increases by increasing the voltage above the breakdown or decreasing the temperature. The afterpulse rate decreases by decreasing the dead time. In the figure (3) display the graph of afterpulse changes.

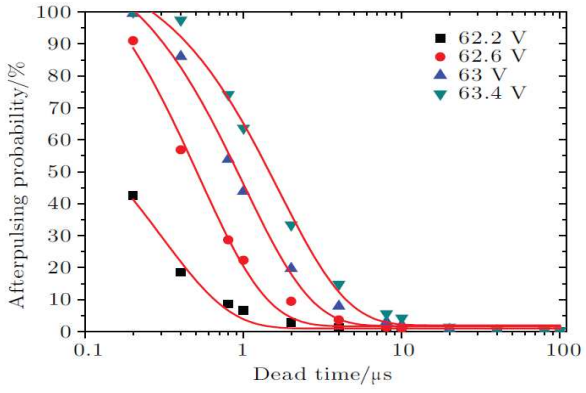


Fig 3. Effective parameter on afterpulse[8]

### B. *Dark Count Rate*

In addition to photon-produced carriers, thermally produced carriers (through regeneration processes inside the semiconductor) can also activate the avalanche process. Therefore, when the SPAD is in complete darkness, pulses can be observed at its output. The average number of counts of these pulses in one second is called the Dark Count Rate (DCR). it is the main parameter in the definition of detector noise[3].

the dark count rate is the average rate of the counts recorded without any incident photons. Dark counting occurs for three reasons: First, false detection events outnumber thermal generation effects. Thermal generation is caused by band-to-band carrier generation or central gap generation. In band-to-band production, carriers are transferred from the capacity band to the conduction band in one step. On the other hand, in the production of the central gap, the carriers are transferred from the capacitance band to the conduction band in two steps. The carriers jump from the capacity band to the middle gap, after some time, they complete their next step by moving from the middle gap to the conduction band. The second reason is that some pulses are recorded at the output of the detector due to the random impact of the photon on the absorption layer. There are different sources of random photons depending on the operating environment. The third reason is that the active area is one of the factors in creating the dark count rate. Therefore, a single-photon detector with a thin active region reduces the dark count rate. the efficiency of the photon detector decreases due to the narrow absorption region construction[3].

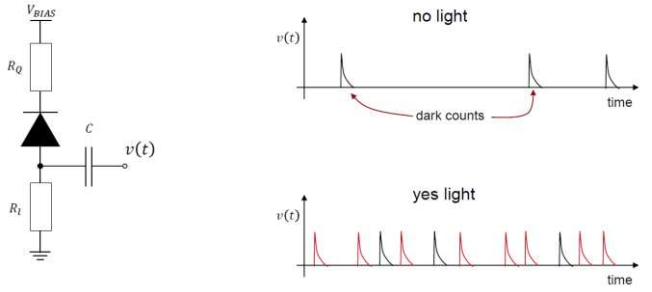


Fig 4. Dark Count Rate with light[3]

Dark pulses generate randomly, and their production interval follows an exponential distribution. The time interval of pulse generation in the dark with units of seconds is expressed by the following equation[3]:

$$\Delta t_{dark} \propto exp\left(\frac{\Delta t}{\tau_{dark}}\right) \quad (5)$$

$\tau_{dark}$: time constant of dark pulse generation

Temperature affects efficiency, gain and, dark count rate[9]. The graph (5) shows the dependence of the dark count rate on temperature. An increase in temperature causes an increase in the dark count rate.

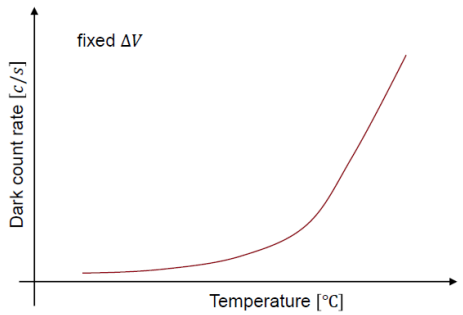


Fig 5. Graph of dependence of dark count rate on temperature[4]

The dark count rate depends on the amount of activating photon at the avalanche threshold level. The higher number of effective photons of the detector cause the less possibility of dark counting error, and the sensitivity of the detector will also decrease. A graph of the effect of increasing the voltage above breakdown on the dark count rate of the detector show in the curve (6). The dark count rate increases exponentially with increasing voltage.

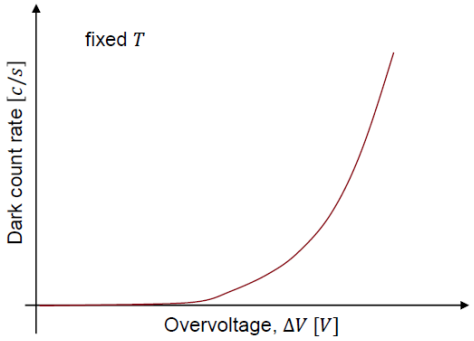


Fig 6: The graph of the relationship between the breakdown voltage and the dark count rate[4]

The measurement of the SPAD primary dark count rate is performed at different temperatures and additional bias voltages due to thermal generation and with the help of carrier field. To eliminate the afterpulse phenomenon (even at low temperatures), all initial DCR measurements are performed with the ON time set to 100ns and the OFF time set to 100µs[10].

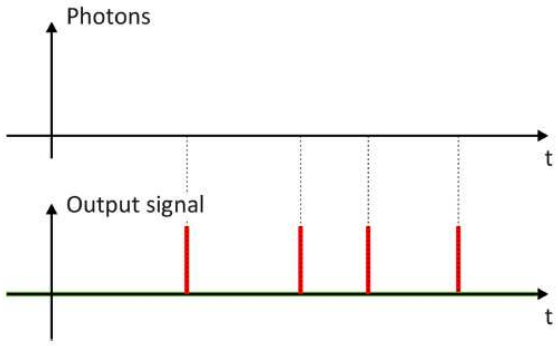


Fig 7: dark count rate[11]

Carriers produced by heat lead to dark pulses. These pulses disrupt the correct pulse detection function. The dark count rate at a fixed gain calculate by the following formula[6]:

$$N_{0.5p.e}(T) \approx AT^{(3/2)} \exp\left[\frac{-Eg}{2KT}\right] \quad (6)$$

*C. Modeling*

The flowchart of the SPAD behavioral model is presented in the figure (8):

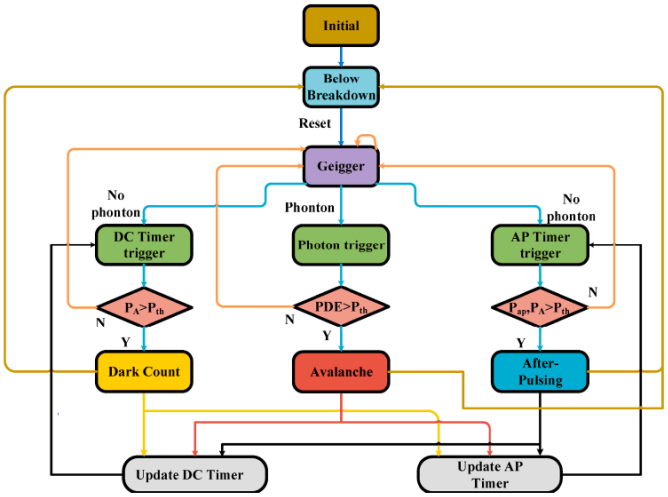


Fig 8. Flowchart of performance analysis and modeling SPAD[12]

There are many models for simulating SPAD elements, such as the traditional model that modeled the SPAD with a voltage source equal to the breakdown voltage of the diode, a series resistor, and a voltage-controlled current. In all these models, the I-V characteristic consider above the linear breakdown voltage. Meanwhile, the measured SPAD I-V characteristic is nonlinear. In order to accurately simulate the behavior of SPAD, need a suitable model is needed[13].

In the figure (9), a more detailed model of SPAD is presented that can model the static and dynamic behavior of the photodiode. This model is obtained using Verilog-A description code:

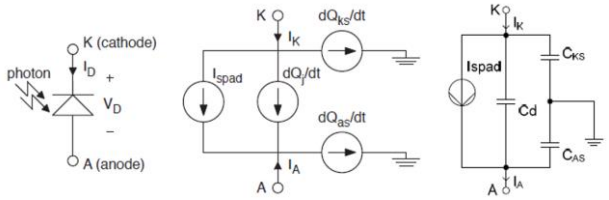


Fig 9. Static and dynamic photodiode model[14]

Verilog-A hardware description code allows analog or mixed-signal devices to be described with varying detail. The ability to describe analog behavior allows the designer to perform modeling and simulation at the system level. Thus, the analog and mixed-signal systems can be described and simulated at a high level at the beginning of the design process to facilitate the whole operation of the chip. Simulation with Verilog-A promotes communication and consistency throughout the design process (from specification to implementation)[15].

```
module spad(a, k, photon);
inout a, k, photon;
branch (k,a)   SPAD;
//////////////////// INITIAL STEP ////////////////////
@(initial_step)
begin
  // Set Breakdown Voltage
  VB = VB0*(1 + VBTC*(T - T0));
  ...
end
////////////////// PHOTON ARRIVAL ///////////////////
if ((V(photon) > PhTh) && (aval == 0))
begin
  aval = 1; // Start the avalanche
  // Schedule next RC events
  deltatcr_i = $rdist_exponential(sdcr_i,taucr_i);
  tcr_i = $abstime + deltatcr_i;
  ...
end
////////////////////// DARK COUNT //////////////////////
...
////////////////////// AFTERPULSING ////////////////////
...
/////////// STATIC AND DYNAMIC CHARACTERISTIC ///////////
Ibrk = (Vn/Rbrk)*ln(1 + limexp(VE/Vn));
Qj  = AD*(phi*Cj0/(1-mj))*pow((1+VD/phi),1-mj);
...
////////////////////// TURN-OFF ////////////////////////
if ((aval == 1) && (Ibrk < Ilat))
begin
  aval = 0;  // Quench the avalanche
  // Update Ilat
  Ilat = $rdist_normal(sdIlat,mIlat,sigIlat);
end
/////////// SET THE  CURRENT CONTRIBUTIONS ///////////
Ispad = Is + aval*Ibrk;
I(SPAD) <+ Ispad + ddt(Qj);
...
endmodule
```

Fig 10. Photodiode simulator code[14]

An example of the output of the simulation circuit present in the figure (11):

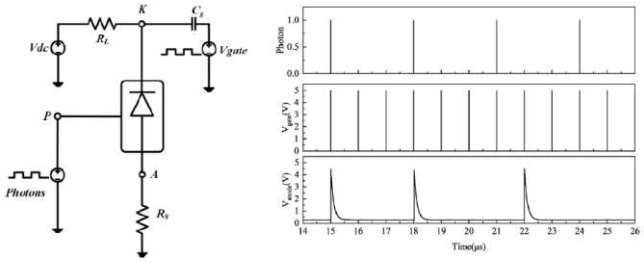


Fig 11. SPAD simulation model[12]

In the figure (12), other models present for SPAD:

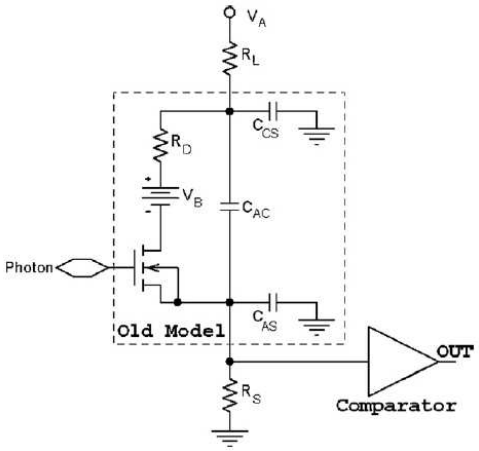


Fig 12. Simple SPAD model[16]

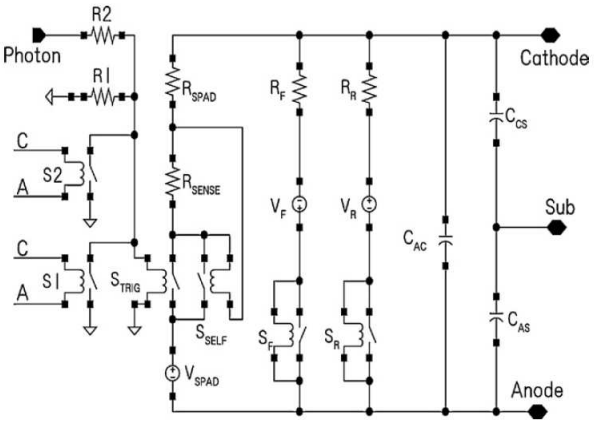


Fig 13. Zappa's model for SPAD[16]

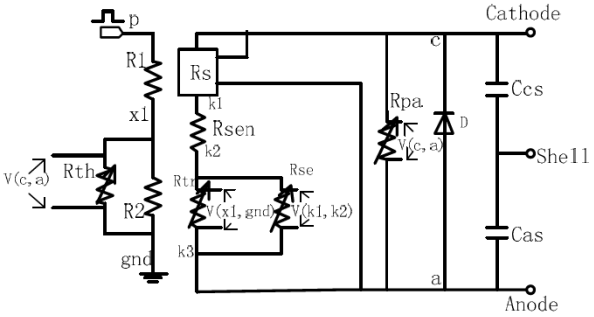


Fig 14. Optimized Zappa's model[17]

The circuit sample simulated in Pspice software show in the figure (15):

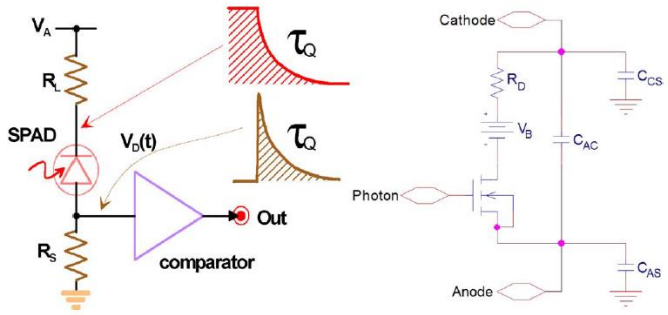


Fig 15. Simulated circuit in Pspice[18]

## III. Presenting the Simulation Method

At first, to add the afterpulse event to the analog model proposed in reference [16], we used the afterpulse generator block. This block creates noise pulses caused by the main pulse in the output of the detector according to the afterpulse occurrence times. The proposed new model was designed and simulated in Pspice software. In the figure (16) And (17), the circuit is designed and the corresponding waveform of its output is presented. This model is not a complete example. it is impossible to randomize the probability of the afterpulse occurrence on it. dark count simulation requires the presence of a randomizer circuit. Consequently, it seems that the design of such a circuit with electronic components, despite its high complexity, does not have optimal accuracy and efficiency. Therefore, researchers should look for a more accurate simulator.

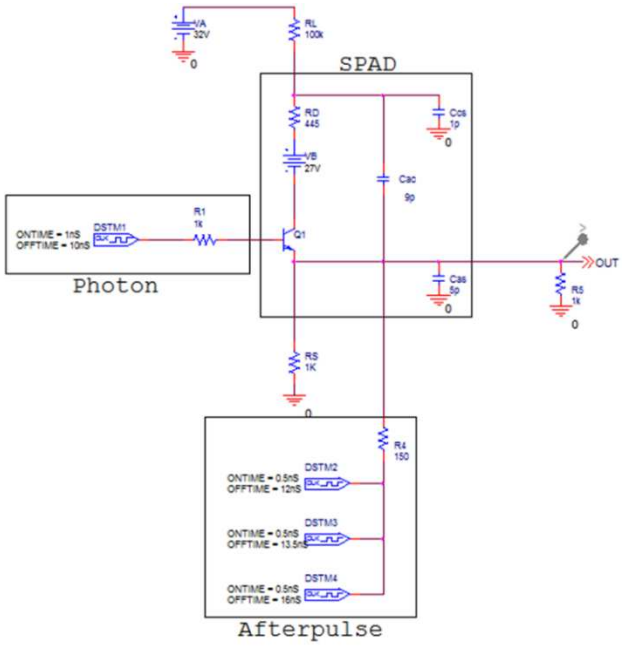


Fig 16. Pspice model for generating afterpulse in SPAD

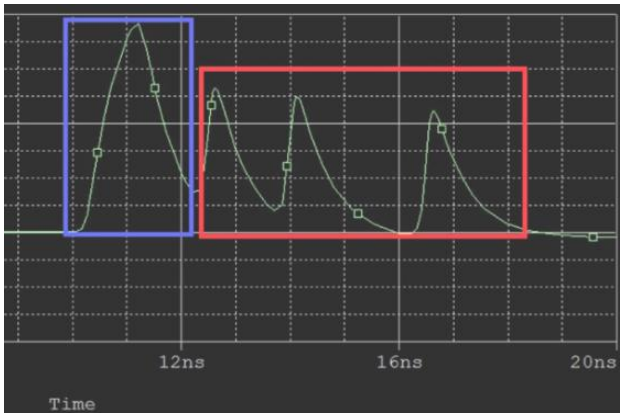


Fig 17. Pspice model output waveform

In the proposed model, a processor capable of executing calculation algorithms is used for simulating dark count and afterpulse counting. In this method, the processor executes the dark counting and afterpulse formulas. The required parameters of the formulas are set as fixed values for the processor. The input of the processor is photon pulses. the output of the processor are dark counting pulses and afterpulse. The parameters are created corresponding to time, temperature and other effective. Those pulses appear in the output of single-photon model.

With the presented method, it is possible to obtain an estimate of the probability of afterpulse occurrence and the number of dark counts for each type of SPAD at different times and temperatures by changing different and effective parameters, and perform a relative analysis and comparison on the performance of single-photon detectors. The optimization and reduction of the dark count and afterpulse can lead to increase in the speed and accuracy of photon detection.

After the implementing of formula (6) on the FPGA chip, within one second, the number of noise pulses will appear next to the photon pulses at random time intervals, as calculated by the dark counting formula. the random block in the FPGA use to create random time intervals. Then, the

random number generator read and putting up pulse times together. By dividing one second by the total number and normalizing the values, the time contribution of each of the random numbers determine from seconds and the dark pulse create at the corresponding time. By this method, dark counting pulses are generated at the output with and without photons at the input,

Now the afterpuls should also be created in the output along with photon pulses and dark counting. For this purpose, Formula (3) is implemented on FPGA for the probability of afterpulse occurrence. The result of calculating this formula is the probability of afterpulse occurrence at different times. In other words, for each received photon, there is a possibility of afterpulse occurrence with the calculated probability. If the calculated probability is close to one, for each photon, there is an expected occurrence of afterpulse. If this probability tends to zero, afterpulse event expect after a more significant number of incoming photons. After calculating the probability of afterpulse occurrence and determining the time of its occurrence, the random generator should be used again. The possibility of afterpulse occurrence is different at various times after photon detection. Afterpulse tends to zero with time.

## IV. Simulation Results

The simulation parameters used for this paper extract from the table (2):

Table 2. of SPAD modeling parameters[12]

| Value | Description | Parameter |
|---|---|---|
| $V_{brk0}$ | Breakdown voltage at room temperature | 69 V |
| $\gamma$ | Temperature coefficient of $V_{brk0}$ | 2.3mV/C° |
| $N_{trap}$ | Trap concentration in multiplication | $2\times10^{14}$ cm$^{-3}$ |
| $N_d$ | Doping concentration in multiplication | $10^{15}$ cm$^{-3}$ |
| $E_{a1}$ | Activation energy of 1st-level trap | 0.0609eV |
| $\tau_{01}$ | The factor of the 1st trap | $4.378\times10^{-7}$ s |
| $E_{a2}$ | Activation energy of 2nd-level trap | 0.0913eV |
| $\tau_{02}$ | The factor of the 2nd trap | $2.412\times10^{-7}$ s |
| $E_{a3}$ | Activation energy of 3rd-level trap | 0.1569eV |
| $\tau_{03}$ | The factor of the 3rd trap | $9.867\times10^{-8}$ s |
| $C_{j0}$ | Zero-bias junction capacitance per unit | 1.19pF |
| $C_{CS}$ | Cathode stray capacitance | 1.69 F |
| $C_{AS}$ | Anode stray capacitance | 2.04pF |
| $W_{mul}$ | Multiplication thickness | 1$\mu$m |
| $W_{ab}$ | Absorption thickness | 1.5$\mu$m |
| $A$ | Effective area | 490.6$\mu$m |

The calculation of the presented formula for the possibility of afterpulse occurrence was done in MATLAB, and the following result was obtained.

```
clc             %%clear
N=3;            %%number of traped electron
T=300;          %%temparture Kelvin (30c)
K=8.617e-5;     %%Boltzmann constant (eV/K)
E1=0.0609;      %%activation energy1 (eV)
E2=0.0913;      %%activation energy2 (eV)
E3=0.1569;      %%activation energy3 (eV)
Q1=4.378e-7;    %%lifetime1 (S)
Q2=2.412e-7;    %%lifetime2 (S)
Q3=9.867e-8;    %%lifetime3 (S)
AREA=490.6e-6;  %%area (m^2)
t1=5e-6;        %%time1 (5us)
t2=2e-5;        %%time2 (20us)
t3=1e-4;        %%time3 (100us)
n=28.6e+15;     %%number of electron after avalanche (1mA=28,6e^18/e^3)
%v=4e-1;         %%electron speed on semiconductor (InGaAs=4000cm^2/VS=0.4m^2/VS)
%A=N*AREA*v;     %%probability of trap occur
A=1e-8;         %%probability of trap occur
A1=A;A2=A;A3=A; %%aprroximation
QQ1 = Q1*(exp(E1/(K*T)));          %%traped electron1 lifetime1
QQ2 = Q2*(exp(E2/(K*T)));          %%traped electron2 lifetime2
QQ3 = Q3*(exp(E3/(K*T)));          %%traped electron3 lifetime3
Pap1 = A1*(1/QQ1)*(exp(-t1/QQ1));  %%afterpulse probability1
Pap2 = A2*(1/QQ2)*(exp(-t2/QQ2));  %%afterpulse probability2
Pap3 = A3*(1/QQ3)*(exp(-t3/QQ3));  %%afterpulse probability3
Pap = Pap1 + Pap2 + Pap3;          %%total afterpulse probability
fprintf('probability of afterpulse is %3.5f ',Pap);%%print answer
fprintf('percent');
```

```
Command Window
fx probability of afterpulse is 0.00086 percent>>
```

Fig 18. MATLAB Implementation of afterpulse formula

The calculation of the formula determine the dark count rate in MATLAB software, and the following result obtain.

```
clc             %%clear
T=300;          %%temparture Kelvin (30c)
K=8.617e-5;     %%Boltzmann constant (eV/K)
Eg=0.03;        %%bandgap (eV)
A=1;            %%arbitrary constant
darkcountrate=A*T^(3/2)*exp(-Eg/2*K*T);          %%darkcountrate (S)
fprintf('darkcount rate is %1.1f ',darkcountrate); %%print answer
fprintf('count per second');
```

```
Command Window
fx darkcount rate is 5194.1 count per second>>
```

Fig 19. MATLAB Implementation of DCR formula


## Acknowledgment

To achieve this idea, the formulas can implement on the FPGA chip. Dark counting and afterpulse can be observed around receiving photons.

Due to the high speed of receiving photons and the need for fast and parallel processing, the processor chip is FPGA type. The selected FPGA model XC3S400 belongs to Xilinx and can replace with other new and advanced models of this company. The FPGA receives its clock from an oscillator with a frequency of 10 MHz and a low error (50 PPM). By embedding the DCM block inside the FPGA chip, it is possible to create square pulses with a frequency higher than this value. The output of the FPGA pulses can directly transfer to the computer. It is possible to read, record and analyze the extracted parameters more easily By connecting the FPGA to the computer through the USB or Ethernet port.


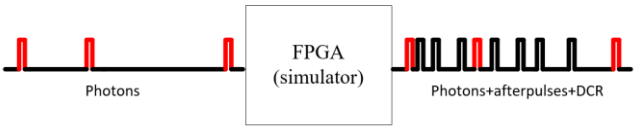


Fig 20. Simulator for afterpulse and DCR

The implementation of afterpulse probability calculation formulas and dark counting pulse generator with VHDL hardware description language on FPGA chip has special

rules, and considerations that are out of the discussion of this article. But with the help of this simulation, it is possible to observe the behavior of SPAD in different conditions of temperature, bias voltage level, type of semiconductor material and other effective parameters, and take action to correct and optimize its behavior.

## REFERENCES


1. *Yu, Y., et al. A review of quenching circuit design based on Geiger-mode APD. in 2018 IEEE International Conference on Mechatronics and Automation (ICMA). 2018. IEEE.*
2. *Pakalapati, M.R.K., Single photon avalanche diode (SPAD) array quenching and a novel quantum random number generator (QRNG). 2019, Florida Institute of Technology.*
3. *Kadhim, A.C., An Approach to Improve Single Photon Detectors for Highly Sensitive Applications. 2018.*
4. *Piatek, S., MPPC & SPAD Future of Photon Counting Detectors. 2019, New Jersey Institute of Technology & Hamamatsu Photonics,: USA. p. 56.*
5. *Yuan, Z., et al., High speed single photon detection in the near infrared. Applied Physics Letters, 2007. 91(4): p. 041114.*
6. *K.K., H.P., MPPC, H.P. K.K., Editor. 2021, HAMAMATSU PHOTONICS K.K.*
7. *Liang, Y. and H. Zeng, High-speed single-photon detection with avalanche photodiodes in the near infrared. Optoelectronics–Materials and Devices. Rijeka: InTech, 2015: p. 213-234.*
8. *Ma, H.-Q., et al., Afterpulsing characteristics of InGaAs/InP single photon avalanche diodes. Chinese Physics B, 2014. 23(12): p. 120308.*
9. *A. Ghassemi, K.S., K. Kobayashi, Multi-pixel photon counter. 2021, HAMAMATSU PHOTONICS K.K.*
10. *Signorelli, F., et al., Low-Noise InGaAs/InP Single-Photon Avalanche Diodes for Fiber-Based and Free-Space Applications. IEEE Journal of Selected Topics in Quantum Electronics, 2021. 28(2): p. 1-10.*
11. *Hofbauer, M., K. Schneider-Hornstein, and H. Zimmermann, Single-photon Detection for Data Communication and Quantum Systems. 2021.*
12. *Xie, S., J. Liu, and F. Zhang, An Accurate Circuit Model for the Statistical Behavior of InP/InGaAs SPAD. Electronics, 2020. 9(12): p. 2059.*
13. *Yang, H.-j., et al. Verilog-A modeling of SPAD for circuit simulations. in International Symposium on Photoelectronic Detection and Imaging 2013: Imaging Sensors and Applications. 2013. International Society for Optics and Photonics.*
14. *Giustolisi, G., R. Mita, and G. Palumbo. Verilog-A modeling of SPAD statistical phenomena. in 2011 IEEE International Symposium of Circuits and Systems (ISCAS). 2011. IEEE.*
15. *FitzPatrick, D. and I. Miller, Analog behavioral modeling with the Verilog-A language. 1998: Springer Science & Business Media.*
16. *Zappa, F., et al., SPICE modeling of single photon avalanche diodes. Sensors and Actuators A: Physical, 2009. 153(2): p. 197-204.*
17. *Huang, D., et al. SPICE modeling for single photon avalanche diode. in International Symposium on Photoelectronic Detection and Imaging 2013: Imaging Sensors and Applications. 2013. SPIE.*
18. *Dalla Mora, A., et al., Single-photon avalanche diode model for circuit simulations. IEEE Photonics Technology Letters, 2007. 19(23): p. 1922-1924.*